

Near-Field Scanning Photocurrent Measurements of Polyfluorene Blend Devices: Directly Correlating Morphology with Current Generation

Christopher R. McNeill, Holger Frohne, John L. Holdsworth, and Paul C. Dastoor*

*School of Mathematical and Physical Sciences, The University of Newcastle,
University Drive, Callaghan, NSW, 2308 Australia*

Received August 31, 2004; Revised Manuscript Received October 20, 2004

ABSTRACT

Near-field scanning photocurrent microscopy (NSPM) measurements probing the relationship between morphology and current generation in photovoltaic devices based on *p*-xylene processed poly(9,9'-dioctylfluorene-*co*-bis-*N,N'*-(4-butylphenyl)-bis-*N,N'*-phenyl-1,4-phenylene-diamine) [PFB] and poly(9,9'-dioctylfluorene-*co*-benzo-thiadiazole) [F8BT] blend films are presented. We find that current generation occurs primarily from within the micron-sized phase-segregated domains, with the PFB-rich phase contributing significantly more current than the surrounding F8BT-rich regions. These results are explained by nanoscale intermixing within the micron-sized domains, with differing extents of intermixing in the PFB- and F8BT-rich domains.

Solar cells based on conjugated polymers offer the possibility of inexpensive, flexible photovoltaics.¹ One route to improving the efficiency of conjugated polymer based solar cells is to blend two polymers with differing ionization potentials and electron affinities, allowing for efficient charge transfer.² Blending is achieved by dissolving the two polymers in the same solvent from which the active semiconducting layer of the device is spin-coated. The blend layers produced thus have donor–acceptor heterojunctions distributed in the bulk of the film, the so-called “bulk-heterojunction”³ architecture and devices fabricated from blend films show enhanced efficiencies over bi-layer architectures.⁴ However, due to their low entropy of mixing, typically the two polymers tend to phase-segregate during the spin-coating process into separated coexisting domains.⁵ Moreover, there is insufficient time during the spin-coating process for an equilibrium state to be reached, namely two separate pure domains, and thus a nonequilibrium morphology is produced as the solvent evaporates. By varying the spin-coating parameters such as solvent, spin-speed, atmospheric conditions, solution and substrate temperature, the degree of phase-separation can be controlled, allowing for device optimization.⁶ In general, an intimate mix between the component polymer networks is desired, since this interpenetrating structure provides both efficient charge transfer and efficient charge transport.

Recently photovoltaic devices fabricated from blends of the polyfluorene-based polymers PFB (p-type) and F8BT (n-type) have attracted considerable attention.^{6–10} Early results found that spin-coating from chloroform produced more uniform films and more efficient devices than films spin-coated from xylene.⁶ In particular, the films spin-coated from chloroform were found to exhibit phase-segregation features on a scale of tens of nanometers, whereas the films spin-coated from xylene were found to exhibit phase-segregation features of the order of tens of micrometers. It would be expected, given an exciton diffusion length of a few nanometers in polyfluorenes,¹¹ that for films where the length scale of the phase-separation appears to vary over orders of magnitude, the device efficiency should vary by a similar magnitude.⁷ Remarkably, however, the efficiency of chloroform-prepared devices with the finer-scale phase-segregation was found to be only 2 to 3 times higher than xylene-prepared devices. Further investigation of the structure of polyfluorene blend films revealed a complex phase-segregated morphology, with nanoscale features existing within the micron-scale structures with the additional possibility of vertical stratification.^{12,13} Indeed, the micron-sized regions initially believed to be rich in one polymer and deficient in the other polymer now appear to contain significant fractions of both materials.¹⁴

The structure of polyfluorene is therefore highly complicated and exhibits phase-separation on a hierarchy of length

* Corresponding author. Tel +61 2 4921 5426; Fax +61 2 4921 6907; E-mail phpd@alinga.newcastle.edu.au.

scales. Furthermore, optimization of these devices requires an understanding of the complex relationships that exist between the film structure and the charge generation and conduction mechanisms. Within each feature, a tradeoff exists between charge generation and transport – finer intermixing promotes charge transfer yet hinders charge transport, while coarser mixing hinders charge transfer yet allows for efficient charge transport. Recently, Snaith et al. have proposed, based on combined photoluminescence quenching, AFM, and photocurrent measurements, that for polyfluorene blend films containing micron-scale phase-segregated domains current generation is optimized for regions close to the interface between these domains, with charges generated within the bulk of either phase contributing weakly to the overall current.⁹ In this paper we present the results of a near-field scanning photocurrent microscopy (NSPM) study with the goal of directly correlating current generation with morphology in xylene prepared polyfluorene blend devices. NSPM is a powerful new technique that allows for two-dimensional mapping of current in fully fabricated organic solar cells.¹⁵ By rastering the light output from a near-field scanning optical microscope tip through a semi-transparent electrode across the solar cell surface it is possible to simultaneously collect height and photocurrent images with a lateral resolution that is governed by the NSOM aperture. For the polyfluorene blend devices studied here, we find that the photocurrent is preferentially generated within each phase and, contrary to previous reports, that there is no evidence for enhanced photocurrent generation at the boundaries between the micron-sized phase-segregated domains.

The technique of near-field scanning photocurrent microscopy has been described in detail elsewhere.¹⁵ Briefly, NSPM measurements were performed using a Nanonics SPM 100 system with 200 nm aperture tips also supplied by Nanonics. The images were collected in contact mode with a 904 nm laser diode used for feedback. Chopped 409 nm laser light was used to excite the solar cells held at virtual short-circuit using a homemade current to voltage converter. The current signal was subtracted from the background noise using a lock-in amplifier (Stanford Research Systems model SR830). Atomic force microscope (AFM) measurements were also separately performed in noncontact mode with 20 nm radius AFM tips to confirm the morphology measured using NSPM and to ensure that no damage was incurred by the surface during imaging.

Poly(9,9'-dioctylfluorene-*co*-bis-*N,N'*-(4-butylphenyl)-bis-*N,N'*-phenyl-1,4-phenylene-diamine) [PFB] and poly(9,9'-dioctylfluorene-*co*-benzo-thiadiazole) [F8BT] (chemical structures shown in Figure 1) were supplied from American Dye Source (Baie D'Urfe, Quebec, Canada) and were purified before use. Molecular weights of the polymers were 32 000 g/mol for PFB and 25 000 g/mol for F8BT (GPC vs PS standards). Solutions of PFB and F8BT were prepared by dissolving in *p*-xylene at a concentration of 25 g/L. 1:1 blend solutions of PFB and F8BT were prepared by combining equal volumes of the 25 g/L solutions of PFB and F8BT.

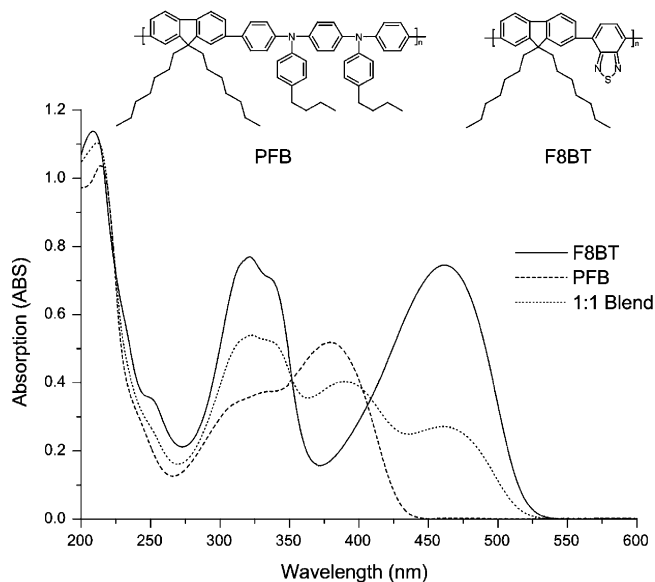


Figure 1. UV–vis absorption spectra of films of F8BT (solid line), PFB (dotted line) and a 1:1 by weight blend film (dashed line). Also shown are the chemical structures of F8BT and PFB.

Films for UV–vis absorption characterization were spin-coated onto fused silica substrates and characterized with a Cary 1E spectrophotometer. The thicknesses of these films were all approximately 100 nm as measured by an Alpha Step 500 surface profilometer.

Photovoltaic devices were fabricated by spin-coating the PFB, F8BT, or 1:1 blend solution onto pre-cleaned indium tin oxide (ITO) substrates to produce films approximately 150 nm thick. These films were transferred to a vacuum system where a calcium electrode capped by a silver layer was deposited at 10^{-5} Pa. Devices studied using NSPM and for photocurrent action spectra measurements through the cathode were deposited with layers of 10 nm of calcium and 20 nm of silver. Otherwise, devices were fabricated with 40 nm of calcium and 60 nm of silver.

Short-circuit photocurrent action spectra were collected using a lock-in amplifier (Ithaco Dynatrac) to measure the short-circuit current signal from the devices when illuminated by chopped monochromatic light from a tungsten halogen lamp passed through a monochromator (Oriel Cornerstone 130). All spectra were corrected for the spectral response of the monochromator and lamp, and when illuminating through a semitransparent Ca/Ag cathode, the spectra were also corrected for the absorption of the metal film.

Figure 1 plots the UV–vis absorption spectra for F8BT and PFB and shows that at a wavelength of 409 nm the absorption coefficients of both polymers are approximately equivalent. As such, any differences in photocurrent generation at this wavelength do not arise from differences in light absorption.

The short-circuit photocurrent action spectra of photovoltaic devices fabricated with pristine F8BT and PFB films, together with that of a 1:1 blend film, are presented in Figure 2a. As expected, the blend device exhibits a significant improvement in efficiency over devices prepared from pristine films of the polymers, consistent with previous

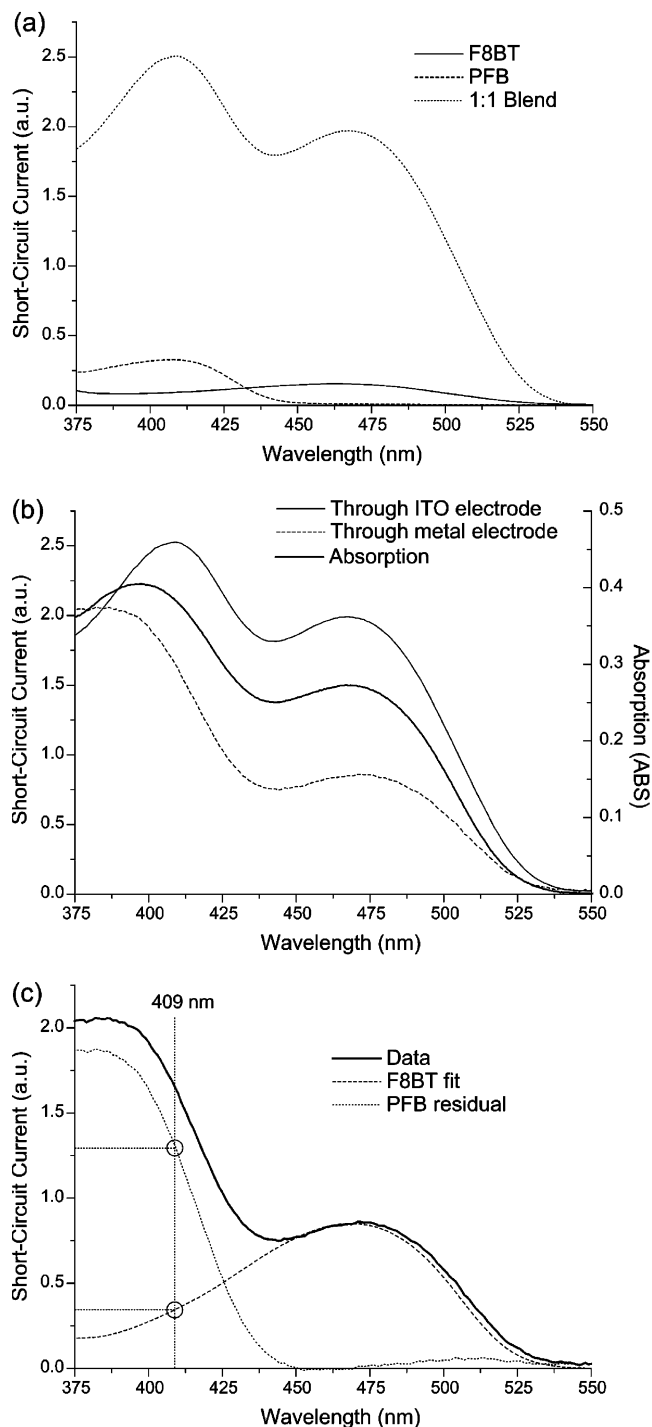


Figure 2. (a) Short-circuit photocurrent action spectra of ITO/F8BT/Ca/Ag (solid line), ITO/PFB/Ca/Ag (dashed line), and ITO/PFB:F8BT/Ca/Ag (dotted line) devices illuminated through the ITO. (b) Short-circuit photocurrent action spectra of the blended ITO/PFB:F8BT/Ca/Ag device for illumination through the ITO electrode (solid, black) semitransparent Ca/Ag electrode (dashed, black) compared to the absorption profile of the blend (gray). (c) Short-circuit photocurrent action spectra of the blended device with illumination through the cathode (solid line) with F8BT component fit (dashed line) and residual PFB component (dotted line).

reports.⁹ Since NSPM measures current from excitation through a semitransparent cathode, rather than through the ITO electrode, it is important to know the spectral dependence of short-circuit current for illumination through a

semitransparent Ca/Ag electrode. Figure 2b shows the spectral response of the blend device for illumination through the ITO electrode and for illumination through the cathode of the same device compared to the absorption profile of the blend film. There are two main differences in the photocurrent action spectra for different electrode illumination. First, there is a shift in the photocurrent peak corresponding to PFB absorption, which is believed to be caused by the filter-effect¹⁶ and can be attributed to the presence of a continuous PFB-rich wetting layer at the ITO electrode.¹² Second, in comparison with the photocurrent spectra of Figure 2b, there is a change in the relative contributions by PFB and F8BT to overall current. While PFB and F8BT harvest similar amounts of current for illumination through the ITO electrode, when illuminated through the cathode, light absorbed by PFB is more than twice as likely to be harvested as light absorbed by F8BT. To determine the relative contributions of PFB and F8BT to the overall current at 409 nm for illumination through the cathode, the data of Figure 2b have been separated into the individual contributions from each polymer (Figure 2c). The contribution of each polymer component to the photocurrent was achieved by fitting UV-vis absorption profile of F8BT to the data shown in Figure 2c. This fit was then subtracted from the overall photocurrent action spectrum. The fact that the resulting PFB residual matches the PFB UV-vis absorption profile of PFB almost identically provides further justification for this approach. By separating the overall current into the contributions due to each polymer, it is calculated from these far-field observations that, for illumination at a wavelength of 409 nm through the cathode, 70% of the current originates from PFB and 30% from F8BT.

An NSPM image and corresponding atomic force microscope (AFM) image measured simultaneously of a 1:1 blend device are presented in Figure 3. The morphology of the 1:1 blend film is consistent with previous reports,^{6,7,9} consisting of micron-sized phase-segregated features and variations in height between phases of approximately 50 nm. The current image indicates that current is preferentially observed within the low height phase, which has been previously identified as being PFB-rich.^{7,13} Current is still generated in the higher phase but has a magnitude that is roughly a quarter of the magnitude of the current generated in the lower phase. Moreover, by measuring the cross-sectional profiles across the phase segregated regions (Figure 4) it is clear that there is no enhancement in photocurrent observed at the boundaries between the micron-sized domains.

As each micron-sized phase covers roughly half of the surface area of the device and the current signal measured in the PFB-rich region is four times that of the current generated in the F8BT-rich region, roughly 80% of the total current for large area illumination through the cathode is generated in the PFB-rich phase. Since each micron-sized domain contains significant amounts of each polymer,¹⁴ the near-field results presented here provide only spatial information about current generation and do not provide local information about which polymer is producing current. Thus

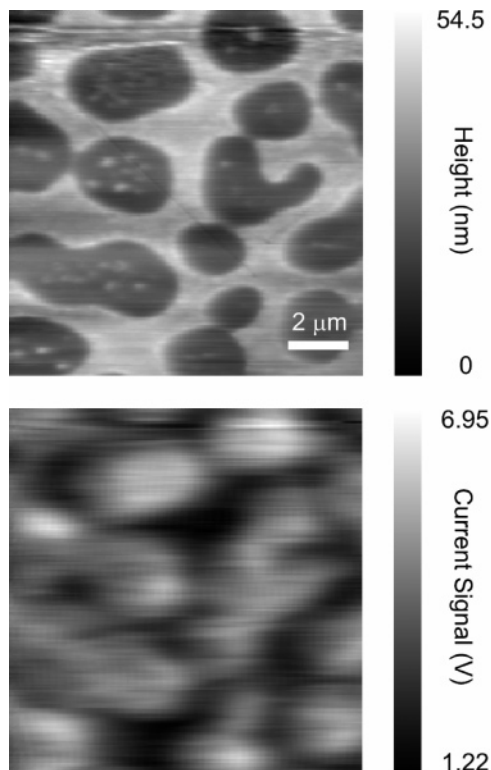


Figure 3. AFM image (top) and corresponding current map (bottom) collected simultaneously of an ITO/PFB:F8BT/Ca/Ag device.

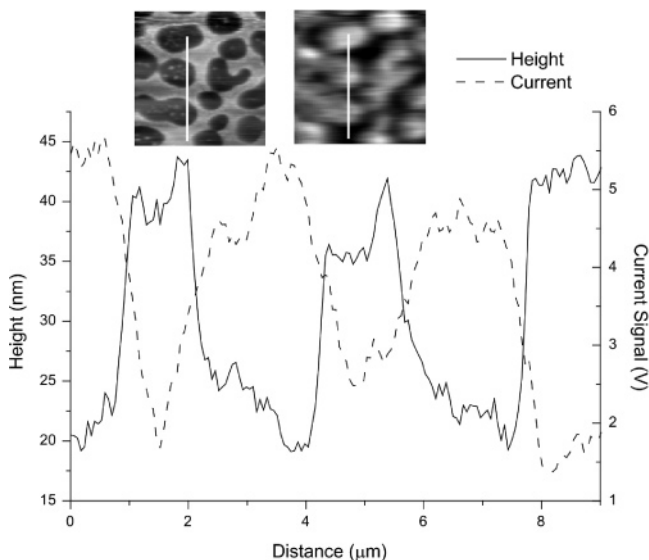


Figure 4. Cross-sectional traces of the AFM image and current map of Figure 3.

while the NSPM observation that 80% of the total current is produced by the PFB-rich region roughly agrees with far-field calculation that 70% of the current originates from absorption by PFB, it cannot be concluded that all the current produced from the PFB-rich region comes from PFB absorption. Further near-field measurements probing at wavelengths at which one polymer absorbs and not the other are necessary to ascertain local information about the relative contributions to current from PFB and F8BT. However, given

that the current is produced from within the micron-sized domains and not at the interfaces between these domains, and given that current is enhanced in the blend device over the pristine devices, it is highly probable that both polymers contribute to the total photocurrent generated from within each micron-sized domain. The higher efficiency of the PFB-rich regions, at least for illumination through the cathode, is attributed to the different relative compositions of the PFB-rich and F8BT-rich phases. Previous work has shown that the PFB-rich region contains more F8BT than the F8BT-rich phase contains PFB.^{9,14} This higher degree of intermixing in the PFB-rich phase results in more efficient charge generation and collection of both n-type and p-type charge carriers. The asymmetry in the F8BT contribution for illumination through the two electrodes is explained by an insufficient concentration of PFB, the p-type polymer, in the F8BT-rich regions for efficient p-type carrier transport in this domain. While there may be sufficient PFB in the F8BT-rich region for charge generation, as indicated by the photoluminescence data of others,⁹ when illumination is through the cathode there is insufficient PFB for efficient transport of holes across the film to the ITO electrode. With illumination through the ITO, on the other hand, the effect of the inefficient collection paths for holes in the F8BT-rich region is not as significant, as the majority of photoexcitations are created near the ITO electrode and the holes do not have as far to travel in order to be collected. Thus, although the F8BT-rich regions have insufficient PFB for efficient p-type carrier conduction, this region can contribute to current for illumination through the ITO electrode when photoexcitations are created predominantly near the ITO electrode and efficient hole collection networks are not as crucial.

The observation that current generation is not enhanced at the boundaries between the micron-sized phase-segregated domains is consistent with near-field photoconductivity measurements made by Riehn et al. on planar gap devices made from F8BT/PFB blends.^{17,18} Riehn et al. found that the photocurrent is essentially constant within the individual blend phases and does not show an enhancement at their boundaries, as might be expected if these were the principal sites for interface-induced exciton dissociation.¹⁸ The observations that photoluminescence¹² and electroluminescence,¹⁹ on the other hand, are enhanced at these domain boundaries in polyfluorene blends also support the results presented here since, in general, areas that have a higher luminescent efficiency have poorer charge generation efficiency. Thus, it appears that the performance of photovoltaic devices made from polyfluorene blend films is determined by the nanoscale mixing of the two components within the micron-sized morphological features and not the micron-sized morphology itself.

These results are likely to have implications also for bulk-heterojunction devices fabricated from poly(*p*-phenylene vinylene) (PPV) and the C₆₀ derivative PCBM.³ Such devices are capable of power conversion efficiencies of up to 3%²⁰ under solar conditions with their performance also depending critically on film morphology.²¹ As with polymer blend films,

depending on the spin-coating conditions, various sized domain structures in PPV/PCBM films are observed. Recent efficiency/nanomorphology investigations by van Duren et al.²² and Hoppe et al.²³ utilizing TEM, SEM, AFM, and photoluminescence spectroscopy have further revealed the nature and influence of PPV/PCBM blend film composition. The results of van Duren et al. and Hoppe et al. have shown that PCBM-rich domains of size 80 nm to 500 nm (80 nm when spin-coated from chlorobenzene and 500 nm from toluene) are formed surrounded by a polymer-rich domain. Similar to the results presented here, we would expect photocurrent to be produced predominantly from within these phase-segregated domains, with the efficiency of each domain determined by the degree of intradomain intermixing. From the observation of unquenched photoluminescence from PCBM in the PCBM-rich domains, indicating photocurrent loss in these areas,²³ we would thus expect photocurrent to be maximized in the surrounding polymer-rich regions. Therefore, for the PPV/PCBM blends as for the polyfluorene blend presented here, overall device efficiency is likely to be determined by the intradomain nanoscale intermixing rather than by the size of the domain structures.

In summary, we have performed NSPM measurements on xylene processed PFB/F8BT blend photovoltaic devices exhibiting micron-sized phase-segregated features. Our NSPM measurements show that current is generated within the bulk and not at the boundaries of the micron-sized phase-segregated features, with the PFB-rich regions producing four times as much current than the F8BT-rich regions for illumination through a semitransparent cathode. Photocurrent action spectra data for illumination through the ITO indicate that the F8BT-rich regions may contribute to current when illuminated through the ITO electrode, but the lack of efficient p-type carrier collection networks, due to insufficient PFB in this phase, prevents efficient harvesting of photogenerated charges when illuminated through the cathode.

Acknowledgment. The Australian Research Council (ARC) is gratefully acknowledged for providing financial support for this project. We thank Jim Cleary for technical assistance. C.R.M. gratefully acknowledges the University of Newcastle for the provision of a research scholarship.

References

- (1) Wallace, G. G.; Dastoor, P. C.; Officer, D. L.; Too, C. O. *Chem. Innovation* **2000**, *30*, 14–22.
- (2) Moons, E. *J. Phys.: Condens. Matter* **2002**, *14*, 12235–12260.
- (3) Brabec, C. J.; Sariciftci, N. S.; Hummelen, J. C. *Adv. Funct. Mater.* **2001**, *11*, 15–26.
- (4) Halls, J. J. M.; Walsh, C. A.; Greenham, N. C.; Marseglia, E. A.; Friend, R. H.; Moratti, S. C.; Holmes, A. B. *Nature* **1995**, *376*, 498–500.
- (5) Bates, F. S. *Science* **1991**, *251*, 898–905.
- (6) Halls, J. J. M.; Arias, A. C.; MacKenzie, J. D.; Wu, W.; Inbasekaran, M.; Woo, E. P.; Friend, R. H. *Adv. Mater.* **2000**, *12*, 498–502.
- (7) Arias, A. C.; MacKenzie, J. D.; Stevenson, R.; Halls, J. J. M.; Inbasekaran, M.; Woo, E. P.; Richards, D.; Friend, R. H. *Macromolecules* **2001**, *34*, 6005–6013.
- (8) Arias, A. C.; Corcoran, N.; Banach, M.; Friend, R. H.; MacKenzie, J. D.; Huck, W. T. S. *Appl. Phys. Lett.* **2002**, *80*, 1695–1697.
- (9) Snaith, H. J.; Arias, A. C.; Morteani, A. C.; Silva, C.; Friend, R. H. *Nano Lett.* **2002**, *2*, 1353–1357.
- (10) Pacios, R.; Bradley, D. D. C. *Synth. Met.* **2002**, *127*, 261–265.
- (11) Stevens, M. A.; Silva, C.; Russell, D. M.; Friend, R. H. *Phys. Rev. B* **2001**, *63*, 165213.
- (12) Chappell, J.; Lidzey, D. G.; Jukes, P. C.; Higgins, A. M.; Thompson, R. L.; O'Connor, S.; Grizzi, I.; Fletcher, R.; O'Brien, J.; Geoghegan, M.; Jones, R. A. L. *Nature Materials* **2003**, *2*, 616–621.
- (13) Kim, J. S.; Ho, P. K. H.; Murphy, C. E.; Friend, R. H. *Macromolecules* **2004**, *37*, 2861–2871.
- (14) Stevenson, R.; Arias, A. C.; Ramsdale, C.; MacKenzie, J. D.; Richards, D. *Appl. Phys. Lett.* **2001**, *79*, 2178–2180.
- (15) McNeill, C. R.; Frohne, H.; Holdsworth, J. L.; Furst, J. E.; King, B. V.; Dastoor, P. C. *Nano Lett.* **2004**, *4*, 219–223.
- (16) Marks, R. N.; Halls, J. J. M.; Bradley, D. D. C.; Friend, R. H.; Holmes, A. B. *J. Phys.: Condens. Matter* **1994**, *6*, 1379.
- (17) Riehn, R., Ph.D. Thesis, University of Cambridge, 2002.
- (18) Richards, D.; Cacialli, F. *Philos. Trans. R. Soc. London A* **2004**, *362*, 771–786.
- (19) Morteani, A. C.; Dhoot, A. S.; Kim, J. S.; Silva, C.; Greenham, N. C.; Murphy, C.; Moons, E.; Ciná, S.; Burroughes, J. H.; Friend, R. H. *Adv. Mater.* **2003**, *15*, 1708–1712.
- (20) Munters, T.; Martens, T.; Goris, L.; Vrindts, V.; Manca, J.; Lutsen, L.; de Ceuninck, W.; Vanderzande, D.; de Schepper, L.; Gerlan, J.; Sariciftci, N. S.; Brabec, C. *Thin Solid Films* **2002**, *403–404*, 247–251.
- (21) Shaheen, S. E.; Brabec, C. J.; Sariciftci, N. S.; Padinger, F.; Fromherz, T.; Hummelen, J. C. *Appl. Phys. Lett.* **2001**, *78*, 841–843.
- (22) van Duren, J. K. L.; Yang, X.; Loos, J.; Bullie-Lieuwma, C. W. T.; Sieval, A. B.; Hummelen, J. C.; Janssen, R. A. J. *Adv. Funct. Mater.* **2004**, *14*, 425–434.
- (23) Hoppe, H.; Niggemann, M.; Winder, C.; Kraut, J.; Hiesgen, R.; Hirsch, A.; Meissner, D.; Sariciftci, N. S. *Adv. Funct. Mater.* **2004**, *14*, 1005–1011.

NL048590C